Received: 19 September 2025 | Revised: 21 November 2025 | Accepted: 24 November 2025

DOI: 10.1002/cjce.70235

RESEARCH ARTICLE

THE CANADIAN JOURNAL OF CHEMICAL ENGINEERING

Microplastics and nanoplastics in water: Improving removal in wastewater treatment plants with alternative coagulants

Sinan Abi Farraj[1,2] | **Mathieu Lapointe**[3] | **Rafael S. Kurusu**[1] | **Nathalie Tufenkji**[1,4]

[1]Department of Chemical Engineering, McGill University, Montreal, Quebec, Canada

[2]Department of Civil and Environmental Engineering, Stanford University, Stanford, California, USA

[3]Department of Construction Engineering, École de Technologie Supérieure, University of Québec, Montréal, Quebec, Canada

[4]United Nations University Institute for Water, Environment and Health, Richmond Hill, Ontario, Canada

Correspondence
Mathieu Lapointe, Department of Construction Engineering, École de Technologie Supérieure, University of Québec, Montréal, QC, Canada.
Email: mathieu.lapointe@etsmtl.ca

Nathalie Tufenkji, Department of Chemical Engineering, McGill University, Montreal, QC, Canada.
Email: nathalie.tufenkji@mcgill.ca

Funding information
Mitacs Accelerate Program; Canada Research Chairs Program, Grant/Award Number: CRC-2022-00274; The Natural Sciences and Engineering Research Council of Canada (NSERC), Grant/Award Number: RGPAS-2019-00117 and RGPIN-2019-04519; The Canada Foundation for Innovation, Grant/Award Numbers: 217263, 36368, 40070, 43152; Graduate Excellence Fellowship (McGill); NSERC and FRQNT, Grant/Award Number: Postdoctoral Fellowships

Abstract

Coagulation, flocculation, and settling have been shown to be important processes to remove micro- and nano-sized plastic contaminants. However, limited research has been conducted to assess how challenging water chemistry characteristics (including water pH and presence of wastewater colloids) and treatment conditions (such as settling time, coagulant type, flocculant type) impact the removal of these contaminants. Our results show that plastic removal declines at higher pH values using conventional alum as a coagulant. Removal of pristine and aged nanoplastics dropped from 64% and 76%, respectively, at pH 7 to below 20% at pH >7.8. Similarly, polyester microfibre removal decreased from 97% at pH 7 to 85% at pH 8.6. Replacing alum with alternative coagulants resulted in improved plastic contaminant removal at pH >7.8 with an average microfibre removal of 94% (aluminium chlorohydrate) and an average nanoplastic removal of 66% (aluminium chlorohydrate + pDADMAC). Quartz crystal microbalance with dissipation monitoring measurements revealed that aluminium chlorohydrate coagulant species yield a thicker deposition layer on negatively charged surfaces compared to alum. Experiments with alternative flocculants revealed that anionic flocculants result in rapid nanoplastic removal, while cationic flocculants can achieve similar removal given sufficient settling times. Results from our study reveal how coagulant and flocculant selection and environmental conditions, including pH and interactions with wastewater colloids, can affect plastic contaminant removal during primary treatment. Our study also revealed that municipalities can enhance nanoplastic and microfibre removal using alternative aluminium-based coagulants under challenging pH conditions.

KEYWORDS

coagulation, contaminants of emerging concern, flocculation, phosphorus removal, plastic pollution, sustainability

1 | INTRODUCTION

The presence of microplastics and nanoplastics in water bodies is expected to increase with the continuous rise in global plastic production. Several studies have already reported the presence of microplastics in various water bodies including oceans,[1,2] estuaries,[3] lakes,[4,5] urban rivers,[6] and groundwater.[7] Of these plastic contaminants, microfibres were found to be the dominant shape of microplastics in wastewater effluents[8] likely originating from laundry machine discharges that contain synthetic textile material.[9–12] Degradation of single-use polypropylene facemasks is also expected to introduce plastic microfibres to natural waters.[13] Recent estimates show that synthetic textiles account for approximately 35% of all primary microplastic release into the environment and constitute the main source of microplastic release in developing countries.[14] Bulk plastic and microplastic litter can further degrade into nanoplastics due to environmental weathering.[15,16] Nanoplastics can be produced following washing and abrasion of synthetic textiles,[17] degradation of polyethylene and polypropylene plastic debris,[18] and mechanical degradation of polystyrene coffee cup lids and expanded polystyrene foam.[19] Nanoplastics are also expected to be released into domestic wastewaters from the use of microbead-containing personal care products which are still being sold in many countries worldwide.[20] Although microplastics, microfibres, and nanoplastics are typically clustered within the same contaminant group, there are important distinctions between these plastic particles beyond shape and morphology. The International Standardization Organization (ISO) defined microplastics as insoluble plastic particles in water that contain at least one dimension between 1 and 5000 μm and defined nanoplastics to have one dimension between 1 and 1000 nm.[21] However, more recent work has called for distinguishing nanoplastics from microplastics not merely by size but also by differences in their transport properties and interactions with colloids.[22,23]

To limit the release of microfibres and nanoplastics into the aquatic environment, it is imperative to assess and improve the ability of existing wastewater treatment plants to remove these contaminants. Since primary settling tanks represent the most common primary treatment process found in wastewater treatment plants,[24] coagulation, flocculation and settling processes present an ideal treatment stage to remove microfibres and nanoplastics. Using alum as a coagulant, Lapointe et al.[25] were able to remove more than 99% of polyester microfibres (105–1325 μm in length) at pH 7. Li et al.[26] showed microfibre removal greater than 90% with 30 mg/L of ferric chloride ($FeCl_3$) from real laundry wastewater and up to 99% microfibre removal with 3 mg/L of polyaluminum chloride. Similarly, Gong et al.[27] were able to achieve more than 95% removal of carboxyl-modified polystyrene nanoplastics using $AlCl_3$, $FeCl_3$, and polyaluminum chloride coagulants at a concentration of 10 mg/L. More than 85% of non-functionalized 50, 100, and 500 nm polystyrene nanoparticles were also removed when polyaluminum chloride was used as a coagulant.[28]

Although these results show high microfibre and nanoplastic removal, it is important to study the effect of influent wastewater conditions such as pH and interactions with wastewater colloids on treatment performance since conventional coagulants are known to be influenced by these conditions. Final pH values can range from 6 to 9.5 according to regulatory standards of wastewater effluent in Québec.[29] Such a change in pH will affect coagulation behaviour as seen with the decline in the removal of polyester microplastics (140 μm) from 89% at pH 7 to 69% at pH 8 when treated with alum.[25] A decrease in polyethylene microplastic removal was also observed by Ma et al. using $AlCl_3$ as a coagulant when the pH was increased from 6 to 8 (27% to 22% removal).[30] The effect of pH on nanoplastic removal with $AlCl_3$ showed a similar behaviour where an increase of initial pH from 8 to 10 resulted in a reduction of nanoplastic removal from 95% to 83.4%.[27] In our previously published work, total suspended solids removal was shown to be an accurate indicator to monitor nanoplastic removal during chemically-enhanced primary treatment for various physico-chemical treatment conditions.[31] In agreement with earlier research, our previous work revealed that changes in operating pH conditions impact the ability of alum to effectively remove both total suspended solids and nanoplastic contaminants. This study builds on our earlier work to better understand the effect of influent wastewater parameters on plastic contaminant removal during coagulation, flocculation and settling. In addition, this work investigates the tools at the disposal of wastewater treatment plant operators (coagulant type, flocculant type, and settling time) to improve removal of this plastic contaminant under challenging treatment conditions.

In this study, the ability of alum to remove nanoplastics and microfibres is tested in varying pH conditions (from pH 7 to 8.6). In addition, we study the ability of alternative coagulants, including aluminium chlorohydrate (ACH) and a mixture of ACH and pDADMAC to remove microfibres and nanoplastics in challenging pH conditions (pH 7.8 to 8.6). Quartz crystal microbalance with dissipation monitoring (QCM-D) was then employed to understand the underlying interactions of coagulants with negatively-charged contaminants. Alternative flocculants including anionic and cationic polyacrylamide flocculants were also tested to highlight the effect of flocculant charge and floc size on nanoplastic

removal. This work contributes to the growing body of literature for nanoplastic and microplastic removal through coagulation and flocculation in two significant ways: (1) the coagulation removal pathways of microfibres, nanoplastics, and phosphorus contaminants are distinguished and (2) the ability of each coagulant to remove plastic contaminants during jar test experiments was related to the coagulant adsorption properties determined through the QCM-D study. The results of these contributions enhance the understanding of the different contaminant removal pathways during coagulation and flocculation and the trade-offs required to ensure optimal treatment of distinct types of contaminants.

2 | MATERIALS AND METHODS

2.1 | Chemicals and materials

Plastic contaminants tested in this study included fluorescent 28 nm carboxylate-modified polystyrene nanoplastics (FluoSpheres F8781, ex/em: 365/415 nm) and microfibres obtained from blended polyester (PEST) textile implemented in previous work.[25] Three aluminium-based coagulants, alum (ALS, Kemira Water Solutions Canada, Inc.), aluminium chlorohydrate (ACH) (PAX XL1900, Kemira Water Solutions Canada, Inc.), and ACH + pDADMAC (PAX XL 3932 J, Kemira Water Solutions Canada, Inc.) were used in this study. Prior work that characterized these coagulants revealed that alum contained ~100% Al monomers (basicity of 0%), while ACH contained ~12% Al monomers and 88% Al_{30} polymer species (basicity of 83%).[32] ACH + pDADMAC coagulant used in this study is composed of 75% ACH and 25% Superfloc C-492 (described below).

Four polyacrylamide (PAM) flocculants were tested including: high MW anionic PAM (aPAM2) (charge density <5%, Superfloc A-100 HMW, Kemira Water Solutions Canada, Inc.), low MW cationic PAM (cPAM1) (charge density ≈ 7%, Superfloc C-492, Kemira Water Solutions Canada, Inc.), low MW cationic PAM (cPAM2) (charge density ≈ 20%, Superfloc C-494, Kemira Water Solutions Canada, Inc.), and low MW anionic PAM (aPAM1) (charge density <5%, Veolia Water Technologies). All stock solutions were stored in the dark at 4°C to prevent potential photodegradation.

2.2 | Jar test preparation

2.2.1 | Synthetic wastewater preparation

Jar test experiments were conducted in synthetic wastewater adapted from the synthetic sewage wastewater recipe from the Organization for Economic Cooperation & Development (OECD).[33] Briefly, a synthetic wastewater concentrate was prepared using 0.8 g of peptone, 0.55 g of meat extract, 0.15 g of urea, 35 mg of sodium chloride (NaCl), 20 mg of calcium chloride ($CaCl_2$), 1 mg of magnesium sulphate heptahydrate ($MgSO_4 \cdot 7H_2O$), and 0.14 g of dipotassium phosphate (K_2HPO_4) dissolved in 500 mL of DI water. To adjust the pH to 8, 300 µL of a 2 M NaOH solution was added to the concentrate. Jar tests containing 250 mL of synthetic wastewater was produced by diluting 20 mL of the synthetic wastewater concentrate with 230 mL of tap water. Each jar test was then spiked with 350 µL of a 40 g/L silica particle suspension (~80% between 1 and 5 µm diameter, S5631, Sigma-Aldrich) to reach an average turbidity of 55 ± 2.3 NTU measured with a TB300 IR turbidimeter (Clear Tech).

2.2.2 | Microfibre preparation

Polyester microfibres used in this study were prepared in earlier work.[25] Briefly, a Ninja blender (~1200 rpm) was used to blend commercial polyester textile (SanMar Canada, ATC, ATC3600Y) for 5 min at 22°C. The blended fibres were sieved with a 250 µm mesh stainless steel sieve resulting in PEST microfibres with a length between 105 and 1325 µm and a width between 12 and 16 µm based on scanning electron microscopy imaging ($n = 30$).[25]

2.2.3 | Nanoplastic preparation

For experiments with pristine nanoplastics, the 28 nm carboxylate-modified polystyrene nanoplastics were pipetted directly from the stock suspension into the synthetic wastewater jar test. For experiments with aged nanoplastics, pristine nanoplastics (1 mL of a 200 mg/L stock suspension) were transferred to a 50 mL Falcon tube containing 20 mL of synthetic wastewater to reach a concentration of 9.5 mg/L. The Falcon tube was left on a shaker at a speed of 50 rpm for 18 h in the dark to preserve the fluorescent properties of the nanoplastics. These nanoplastics are hereafter referred to as aged nanoplastics.

2.2.4 | Spiking synthetic wastewater with plastic contaminants

Nanoplastics (either pristine or aged) and microfibres were added to synthetic wastewater jar tests based on the following procedures. Pristine nanoplastics were added to 250 mL of synthetic wastewater to achieve a

concentration of 0.8 mg/L (1 mL of a 200 mg/L stock suspension). Microfibres were added to the jar to achieve a number concentration of 1000 microfibres/L (2.31 mL of a stock suspension of 108 ± 11 microfibres/mL). For experiments with aged nanoplastics, 20 mL of synthetic wastewater containing the aged nanoplastics (9.5 mg/L) were added to 230 mL of synthetic wastewater to achieve a nanoplastic concentration of 0.8 mg/L.

2.3 | Jar test procedure

After spiking the synthetic wastewater with the plastic contaminants, the pH of the suspension was adjusted by adding 2 M NaOH and 1 M HCl before the onset of the jar test procedure to achieve the target pH. To begin the jar test experiment, the coagulant was added at a concentration of 5.45 mg Al/L and mixed for 2 min at a speed of 110 rpm. The concentration of alum was optimized to reach a turbidity value less than 10 NTU after 3 min of settling in jar tests containing synthetic wastewater spiked with polyester microfibres at a concentration of 1000 microfibres/L (Figure S1). This was followed by a 2 min flocculation period with the addition of 0.4 mg PAM/L at the same speed of 110 rpm. Half of the total dosage of PAM (0.2 mg PAM/L) was added at the onset of flocculation, while the other half was added at mid-flocculation to avoid floc breakage.[25] Stirring was stopped after the flocculation period and samples were collected at 30 s and 3 min of settling from a depth of 3 cm below the water surface level. Results obtained after 30 s of settling reveal the ability of the coagulation-flocculation process to remove contaminants rapidly and effectively which can impact the operating cost of the process. Results after 3 min of settling reveal the removal of contaminants when the majority of flocs have been settled.

2.4 | Nanoplastic, microfibre, and phosphorus concentration measurements

The initial and final concentrations of pristine and aged nanoplastics were determined by measuring fluorescence intensity (Spark microplate reader, Tecan) with a corresponding calibration curve in synthetic wastewater (linear relation, $R^2 > 0.98$, Figure S2). To measure microfibre removal, 100 mL samples were collected from each jar test by pouring the treated water into a graduated cylinder after 3 min of settling. The sample was then filtered with 5 µm mixed cellulose ester membranes (MF-Millipore®, membrane filter) and the number of microfibres on the membranes were counted using a stereomicroscope (Olympus, model SZX16). Samples with high turbidity (>30 NTU) can result in build-up on the membrane during filtration which can impede microfibre counting. Three to five membranes were used to filter these 100 mL samples to avoid membrane fouling and particle build-up which can hinder the visualization and counting of microfibres.

To measure the phosphorus concentration after treatment, 50 mL of treated water from each jar was filtered with a 0.45 µm mixed cellulose ester membrane (MF-Millipore®, membrane filter). In addition to plastic contaminant removal, this study measured the impact of coagulant type on phosphorus removal. Since phosphorus is an important contaminant for WWTPs,[34,35] this study explores any potential tradeoff between plastic contaminant removal and phosphorus removal. The concentration of phosphorus was measured in triplicate by an accredited testing laboratory, Eurofins (Québec, Canada), using inductively coupled plasma mass spectrometry (ICP-MS, ICAP, Thermo Fisher Scientific). The initial concentration of soluble phosphorus in untreated synthetic wastewater is 5.0 ± 0.5 mg/L based on the recipe implemented in this study.[36,37] Measurements were taken for at least three separate jar tests to ensure the reproducibility of the nanoplastic fluorescence measurement, microfibre visual counting, and phosphorus concentration measurement.

2.5 | Floc imaging and sizing

To measure floc sizes, 2 mL samples were collected 10 s before the end of the flocculation period at a distance 3 cm below the water surface. To collect the sample, the tip of a 5 mL pipette was cut ~1 cm from the edge for a wider pipette tip opening to ensure minimal impact on the floc structure. An inverted fluorescence microscope (Olympus, model IX71) with brightfield imaging was then used to take optical images of the flocs. Analysis of floc sizes was performed with ImageJ software for more than 60 flocs total (at least 20 flocs per jar test from three separate jar test experiments). The size of the floc was calculated assuming an ellipse shape with an equivalent diameter = $(L \cdot W)^{0.5}$ where L and W are the length and width of the floc.[38] For SEM images, settled flocs were collected and placed on carbon tape, dried for 24 h, and coated with 4 nm of platinum (Leica Microsystems, EM ACE600 High Resolution Sputter Coater). The electron microscopy images (FEI Quanta 450 environmental scanning electron microscope) were obtained at 5 kV (secondary electrons), while the elemental analysis obtained by energy-dispersive X-ray spectroscopy was performed at 10 kV. Elemental mapping was analyzed with EDAX Octane Super 60 mm^2 SDD and TEAM EDS Analysis System.

2.6 | Dynamic light scattering and zeta potential measurements

The hydrodynamic size and zeta potential of nanoplastics were measured using a Zetasizer Ultra (Malvern Panalytical). Nanoplastics (28 nm carboxylate-functionalized nanoplastics; 100 ppm concentration) were suspended in DI water at 25°C containing 0.66 mmol NaCl/L which is equivalent to the ionic concentration of synthetic wastewater. Stock suspensions were prepared in four pH conditions (pH 7.0, 7.5, 8.0, and 8.5) by adding NaOH (1 M) and HCl (1 M) to adjust the pH. Three separate samples were measured at each pH condition. For each sample, the hydrodynamic size is reported as an average of three dynamic light scattering z-average measurements while the zeta potential is reported as an average of at least six measurements.

2.7 | Quartz crystal microbalance with dissipation monitoring (QCM-D) measurements

2.7.1 | QCM-D sample preparation

QSense Explorer was used to study the affinity of the three coagulants to a 5 MHz AT-cut crystal with silica-coated surface (QSX 303, QSense). All three coagulant samples were prepared to reach a final concentration of 5.45 mg Al/L in 250 mL of pre-filtered (0.2 μm) DI water. To control the pH of the sample, NaOH (0.5 mol/L) and HCl (1 mol/L) were added to reach a pH of 7 ± 0.2 for alum and 8.5 ± 0.2 for ACH and ACH + pDADMAC.

2.7.2 | QCM-D measurement procedure

To assess the affinity of the three coagulants to the sensor, the frequency shifts (Δf) and dissipation shifts (ΔD) were measured for each coagulant. To establish a baseline measurement for Δf and ΔD, a peristaltic pump was first used to flow pre-filtered DI water with the same adjusted pH as the selected coagulant at a rate of 100 μL/min for 5 min. Then, the coagulant sample (5.45 mg Al/L) was pumped into the flow module at an identical flowrate of 100 μL/min. The Δf and ΔD responses of the crystal to the coagulant were reported for the third overtone ($n = 3$). It should be noted that the frequency shift obtained from the QCM-D (Q-Sense) is already normalized when using standard software settings such that $\Delta f_{(n)} = \Delta f_n/\mathrm{n}$. Three separate experiments were conducted for each coagulant to measure frequency shift and dissipation shift as a function of time (Figure S3).

2.7.3 | Sensor and chamber cleaning procedure

Before each measurement, the silica-coated sensor (QSX 303, QSense) was cleaned three times in 0.2 μm pre-filtered DI water, soaked in 0.2 μm pre-filtered Hellmanex (1%) and bath sonicated for 20 min.[39] Following sonication, the sensor was rinsed 10 times with DI water, 3 times with ethanol and dried under nitrogen gas. Finally, the sensor was exposed to UV/ozone treatment for 45 min (UV chamber, Bioforce Nanosciences). To clean the crystal, chamber, and tubing after each measurement, pre-filtered DI water was pumped into the chamber for 5 min, followed by 1% Hellmanex for 1 min, and then DI water for five additional minutes.

2.8 | Statistical analysis

Two-sample t-test with equal variance was performed in MATLAB[40] to determine whether the means of two treatment conditions differed significantly. This was applied to compare the coagulant performances for different treatment conditions and varying contaminant types. A p-value of less than 0.05 was considered statistically significant.

3 | RESULTS AND DISCUSSION

3.1 | Effect of pH on microfibre and nanoplastic removal using alum as a coagulant

A maximum observed nanoplastic removal of 64% ± 3% was reached at pH 7 with an alum concentration of 5.45 mg/L for samples collected 30 s after stirring was stopped at the end of the (2 min) flocculation period (30 s of settling) (Figure 1A). Nanoplastic removal was observed to be largely impacted by increasing pH with a measured nanoplastic removal below 10% for all pH values greater than 8. To study the effect of wastewater colloid interactions with nanoplastics prior to physicochemical treatment, pristine nanoplastics were stabilized in synthetic wastewater for 18 h. The stabilization period is introduced in this study to mimic the potential interactions between wastewater colloids and nanoplastics that occur during nanoplastic transport in sanitary sewer systems (referred to as aged nanoplastics). Following coagulation with alum, nanoplastic removal at pH 7 is seen to be significantly greater for aged nanoplastics compared to pristine nanoplastics (76% ± 4% vs. 64% ± 3% respectively, $p = 0.039$, Figure 1B). At higher pH values, the

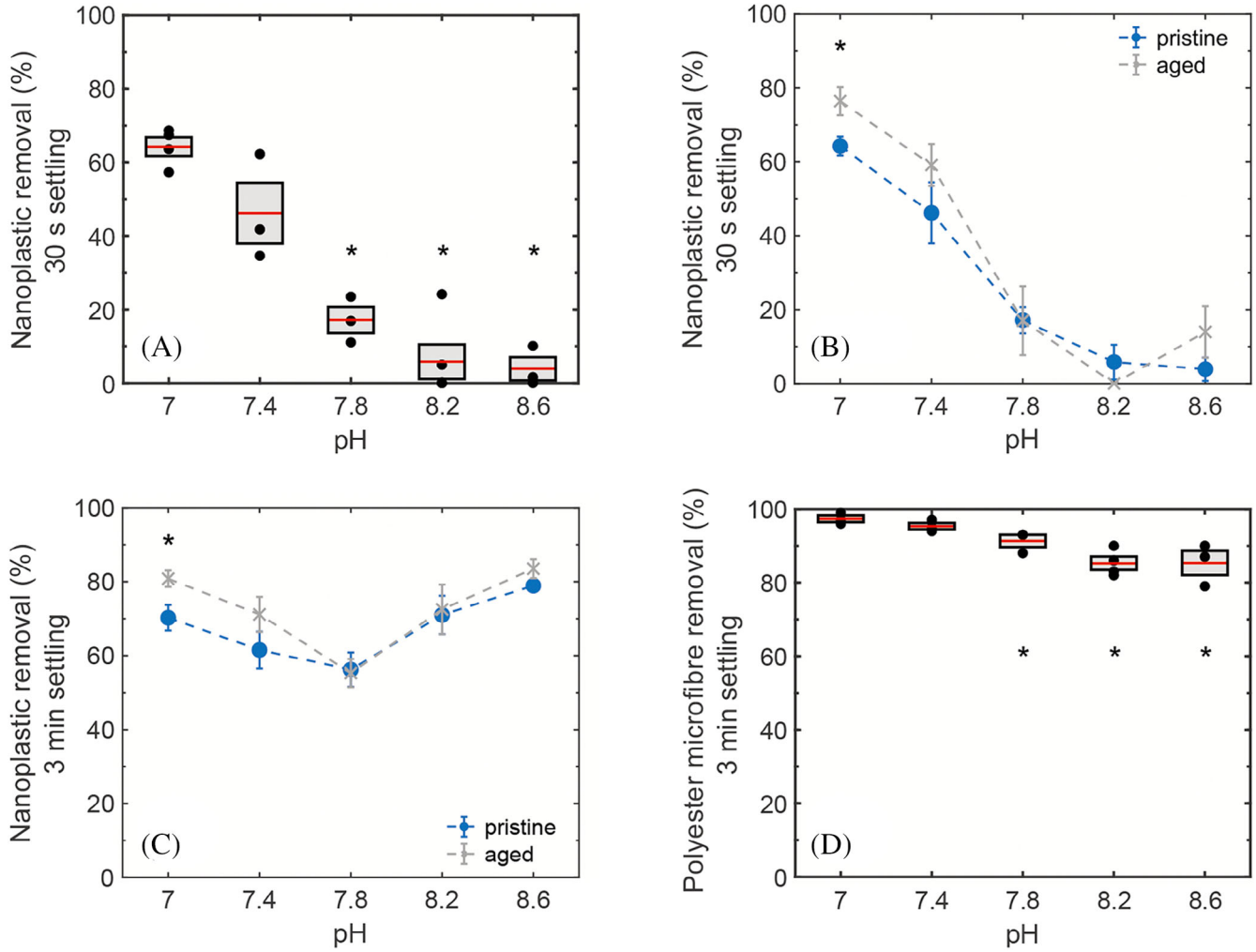

FIGURE 1 (A) Removal of pristine nanoplastics as a function of final pH conditions of water after 30 s of settling. Removal of pristine (circle) and aged (star) nanoplastics after (B) 30 s of settling and (C) 3 min of settling. (D) Removal of polyester microfibres after 3 min of settling. Conditions: 5.45 mg Al/L of alum, 0.4 mg/L of anionic PAM (aPAM1) (very low anionic charge density, high molecular weight); 2 min of coagulation and 2 min of flocculation at 110 rpm. For (A, D), each datapoint represents a single jar test with the red line and the grey box indicating the mean and the standard error of all jar tests at that condition, respectively. For (B, C), each data point represents an average of at least three separate jar test results and the error bar indicates standard error. *Indicates statistically significant difference ($p < 0.05$; two sample *t*-test) between (A, D) pristine nanoplastic removal at pH 7 and other pH values or between (B, C) pristine nanoplastic removal at the same pH value. Selected data in (A–C) are sourced from the same dataset as Abi Farraj et al.[31]

aged nanoplastics showed the same decline in removal to reach values lower than 20% at all pH values above 8, as noted previously for pristine nanoplastics.

The lower nanoplastic removal in more alkaline conditions can be explained by the effect of pH on the behaviour of alum during coagulation. When alum is used as a coagulant, colloid destabilization can occur through charge neutralization or sweep flocculation. Given the alum dose of 60 mg/L used in this study, sweep flocculation is expected to be the dominant removal mechanism across the pH range of 7–9.[41] In this flocculation regime, the concentration of the added alum is beyond the solubility limit which results in excess alum hydrolyzing to amorphous $Al(OH)_3$ that entraps the colloids within the precipitating aluminium hydroxide.[41] In alkaline conditions, hydrolyzed alum species are known to be negatively charged. Although the charge of $Al(OH)_3$ is positive at a pH of 7–8, the charge of $Al(OH)_3$ becomes weakly negative at pH values greater than 8.[42] In addition, the concentration of negatively charged $Al(OH)_4^-$ increases with pH.[41] The excess of negatively charged soluble alum species could impact their affinity to negatively charged colloids in the wastewater as well as the anionic polyacrylamide used in the flocculation stage.[43] This increase in electrostatic repulsion between coagulation species and flocculants and contaminants can possibly explain the smaller flocs formed at higher pH values. Floc images revealed that flocs formed at pH 7 had an

average size of 541 μm compared to 296 μm for flocs formed at pH 8 (Figure S4). In addition, roughly 26% of flocs produced at pH 7 were larger than 750 μm compared to only 1% for pH 8. Therefore, nanoplastic removal in samples measured after 30 s of settling at pH 8 is expected to be lower since these smaller flocs require a longer time to settle.

Nanoplastic removal after 3 min of settling takes into account any nanoplastics removed with smaller flocs that take longer to settle (Figure 1C). Although a significant decline in pristine nanoplastics removal was observed at the lower settling time (30 s) with alum, the results after 3 min show no significant difference in removal between pH 7 and higher pH levels ($p > 0.05$, two sample t-test). This result suggests that nanoplastics are entrapped in the smaller flocs produced at higher pH. Interestingly, the lowest nanoplastic removal for both pristine and aged nanoplastics after 3 min of settling is seen at pH 7.8. Removal of aged nanoplastics at pH 7.8 is significantly lower than removal at pH 7 and 8.6 ($p = 0.002$ and 0.004, respectively). Zeta potential and DLS measurements reveal that the polystyrene nanoplastics maintain a negative surface charge (< -30 mV) with minimal aggregation across the pH range of 7.0–8.5 (Figure S5). Therefore, the greater removal at pH values greater than 8 can be due to the improved affinities that nanoplastics have with Al polynuclear species that form in higher pH conditions (e.g., Al_2, Al_3, Al_{13}).

On the other hand, microfibres showed a significant difference in removal at varying pH conditions after 3 min of settling. At an optimal pH of 7, coagulation with alum achieves high removal of polyester microfibres (97% ± 1%) (Figure 1D). This result agrees with earlier coagulation studies that showed a 99% polyester fibre removal (mean floc diameter of 977 ± 36 μm) when alum (2.73 mg Al/L) and PAM (0.3 mg/L) were added as a coagulant and flocculant, respectively.[25] Similarly, Shahi et al.[44] observed a 81.8% removal of elongated polyethylene (10–100 μm) with alum (30 mg/L). The high fibre removal was attributed to the shape of microplastics with a recent meta-analysis revealing that microplastics shaped like fibres have the highest removal in the coagulation and sedimentation process.[45] However, increasing the pH of wastewater in this study led to a decrease in microfibre removal reaching 85% ± 3% removal at a pH of 8.6 ($p = 0.024$ compared to pH 7). A similar decline in removal was also reported for polyester microspheres (140 μm) with a reduced removal of 69% at pH 8 when alum was used as a coagulant.[25]

The different effects of pH conditions on nanoplastic and microfibre removal after 3 min of settling can be explained by the attachment process of each contaminant. In the sweep coagulation regime, the removal of microfibres is expected to be dominated by the attachment of microfibres to flocs.[13,25] As can be seen in the SEM image (Figure 2), the microfibre appears to be enmeshed in the aluminium-based floc along with silica particles that constitute the inorganic colloids in the synthetic wastewater (Figure S6). The effect of pH on the removal of microfibres can be attributed to the size and charge of the produced flocs. Due to the length of microfibres (160–1500 μm), it is expected that microfibres are less likely to enmesh with smaller flocs produced at pH >8 than the larger flocs produced at pH <8. The effect of floc size on microplastic removal was also shown in the study by Lapointe et al.[25] When the floc size was reduced by lowering the dose of flocculant, a significant decrease in the removal of 140 μm microspheres was observed, while the removal of smaller 15 μm microspheres was not affected. Similarly, in this study, the smaller flocs impacted the removal of microfibres but not the smaller-sized nanoplastics. This difference in removal suggests that sweep flocculation with smaller flocs is less effective for removing microfibres. The different removal

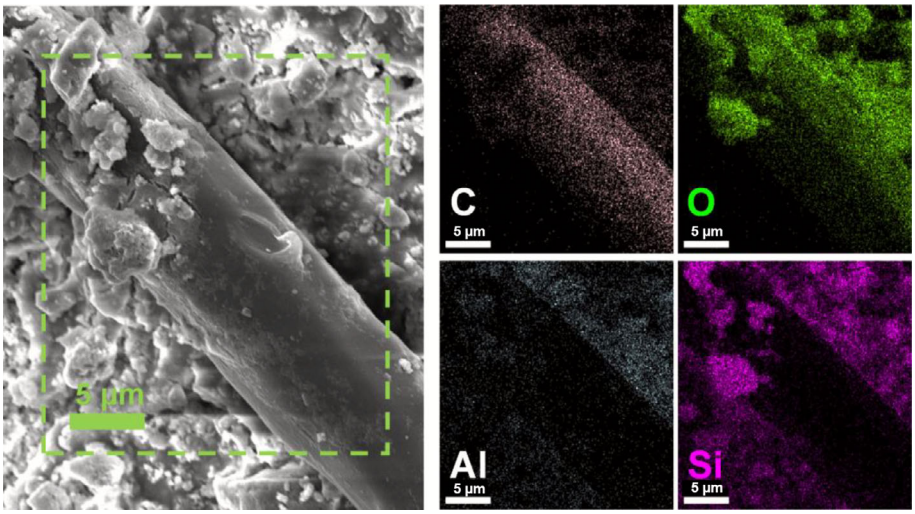

FIGURE 2 Scanning electron microscope image of polyester microfibre embedded in a settled floc and the corresponding EDS elemental mapping showing the presence of carbon, oxygen, aluminium (as Al hydroxides obtained from alum), and silicon (scale bars = 5 μm). The brightness of the energy dispersive X-ray spectroscopy (EDS) elemental mapping images was increased by 50% to enhance the visibility of the location of detected elements.

behaviour between microfibres and nanoplastics further supports the need to differentiate between the unique physicochemical behaviours of nanoplastics and microplastics.[22,23] In addition, the weakly negative charge of $Al(OH)_3$ that precipitates at pH values greater than 8 can result in electrostatic repulsion with the negatively charged polyester microfibres resulting in a lower likelihood of microfibre enmeshment in the aluminium hydroxide based flocs.

3.2 | Microfibre and nanoplastic removal with alternative coagulants in alkaline conditions

Aluminium chlorohydrate (ACH) is a prehydrolyzed aluminium-based coagulant containing positively charged polymeric aluminium species including $[AlO_4Al_{12}(OH)_{24}(H_2O)_{12}]^{7+}$ and $[Al_{30}O_8(OH)_{56}(H_2O)_{24}]^{18+}$, known as Al_{13} and Al_{30}, respectively.[46] In contrast to monomeric Al hydroxide species from alum, the hydrolyzed cationic species formed from ACH are stable at a wider pH range.[32] Using ACH as a coagulant resulted in a significantly greater nanoplastic removal compared to alum at all pH values greater than 7.8 ($p < 0.05$) for samples collected after 30 s of settling (Figure 3A). The introduction of cationic polyaluminum species is seen to improve the removal of nanoplastics due to the improved floc structure produced at that pH range as well as a possible enhanced charge neutralization of colloids. It is worth noting that the nanoplastic removal significantly decreased for ACH at higher pH conditions ($p < 0.05$ for data points compared to pH 7.8). A previous study has shown that the zeta potential of coagula formed by the coagulation of Al_{13} and Al_{30} species decreases at high pH, noably due to the increased negativity of particulate contaminants.[47] This reduction in coagulant charge neutralization capacity can explain the decrease of nanoplastics removal with ACH at higher pH conditions. The role of the cationic species in improving nanoplastic removal at short settling times is further supported when pDADMAC is introduced with ACH. Nanoplastic removal at pH 8.2 is seen to be significantly greater for ACH + pDADMAC at 75 ± 3% removal compared to ACH at 42 ± 4% ($p < 0.05$). Therefore, the addition of cationic pDADMAC is seen to compensate for the loss of cationic charge on the polyaluminum nuclear species to ensure the rapid removal of nanoplastics.

For samples collected after 3 min of settling, ACH as well as ACH added in combination with pDADMAC significantly improve nanoplastic removal compared to alum at pH 7.8 ($p = 0.035$ and $p = 0.002$, respectively; Figure 3B). In addition, nanoplastic removal with ACH + pDADMAC is seen to be significantly greater than ACH alone ($p = 0.046$ at pH 7.8). Therefore, at pH conditions of 7.8, the cationic pDADMAC species play an important role in contaminant removal particularly through destabilizing the nanoplastic contaminants. For pH values greater than 8.2, there was no significant difference in nanoplastic removal between alum, ACH, and ACH + pDADMAC. This finding supports the hypothesis that in highly alkaline conditions, sweep flocculation by alum compensates for the loss in cationic species and results in similarly high nanoplastic removal given enough settling time.

Microfibre removal also revealed significant improvement when polynuclear aluminium coagulants are added. Jar test experiments show that ACH maintains high removal of microfibres in alkaline conditions and offers a significantly greater removal than alum (Figure 3C). This result shows that cationic species that are stable at higher pH values can improve removal of negatively charged colloids and microfibres. However, introducing additional cationic species to the coagulant via pDADMAC addition resulted in a wide variation in microfibre removal at high pH values. Microscopy images reveal that the low microfibre removal can be attributed to small flocs that are floating on the surface of the water (Figure S7). These small flocs are suspected to form due to the strong cationic nature of pDADMAC as was later confirmed in the QCM-D analysis. As mentioned earlier, microfibre removal was determined by counting the number of microfibres left in suspension after the prescribed settling time. Since this concentration measurement includes any flocs suspended near the surface, the incorporation of microfibres into these smaller floating flocs can explain the lower observed removal. An earlier study by Rajala et al.[48] similarly observed that cationic (polyamine) coagulant can result in small floc sizes in certain treatment conditions. Under these conditions, the cationic polymer produced small aggregates that remained in suspension and resulted in lower microsphere removal.

Wastewater operators are facing regulatory drivers to reduce phosphorus concentrations in effluent streams as it has been shown to deteriorate water quality and result in harmful algal blooms. In this study, the coagulants' mechanisms of phosphorus removal are compared to their mechanisms of plastic contaminant removal. Our results reveal a potential tradeoff between nanoplastic removal and phosphorus removal with alum. Although alkaline conditions did not appear to affect nanoplastic removal with alum at long settling times, there was observed decline in phosphorus removal (Figure 3D). Final phosphorus concentration with alum achieved a concentration less than 1 mg/L at pH 7 (initial concentration = 5.0 ± 0.5 mg/L). As the pH increased,

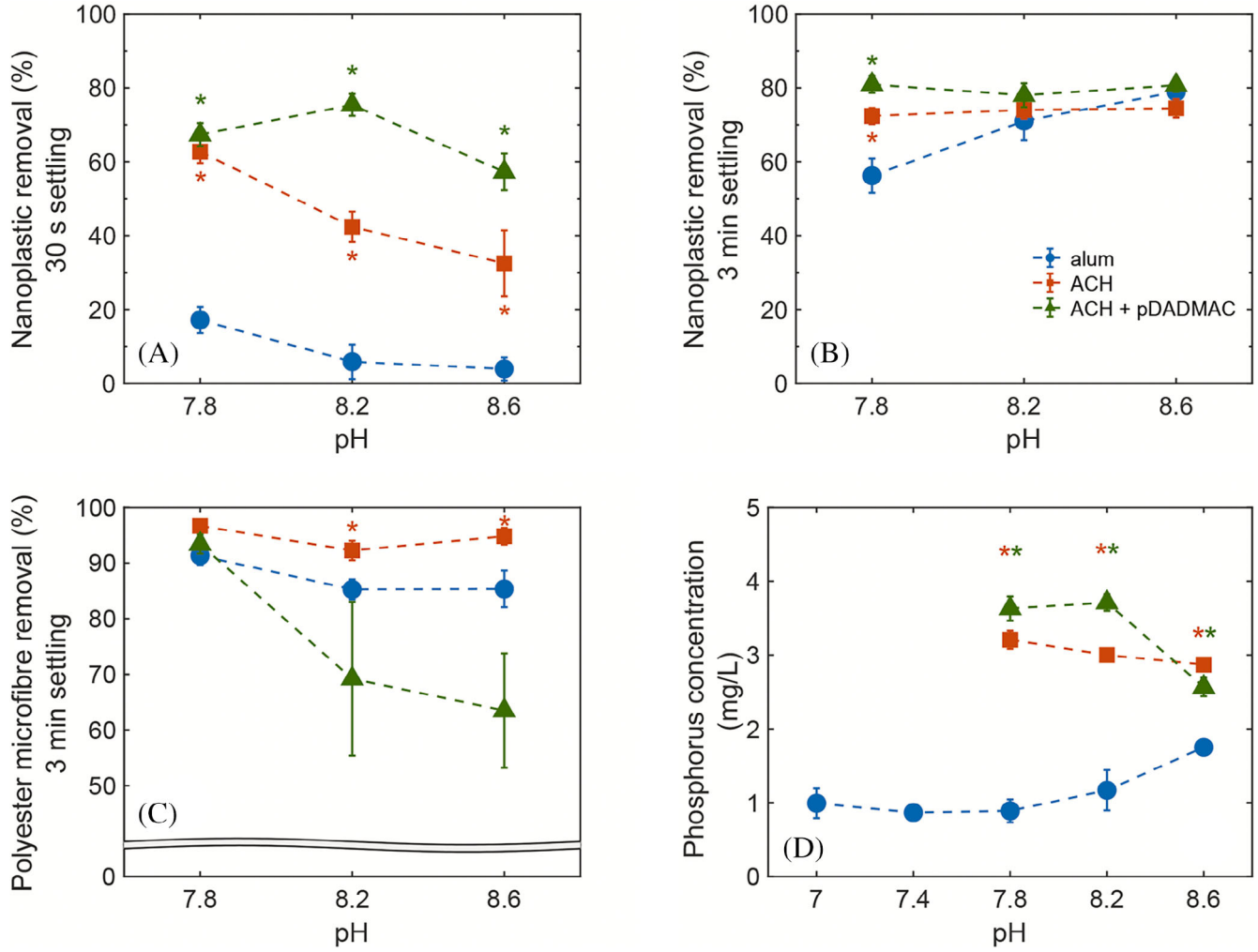

FIGURE 3 Comparison between alum (circle), aluminium chlorohydrate (ACH) (square) and ACH + pDADMAC (triangle) coagulants on the (A) removal of pristine nanoplastics after 30 s of settling, (B) removal of pristine nanoplastics after 3 min of settling, (C) removal of polyester microfibres after 3 min of settling, and (D) final phosphorus concentrations. Conditions: 5.45 mg Al/L of coagulant; 0.4 mg/L of anionic anionic PAM (aPAM1) (very low anionic charge density, high molecular weight); 2 min of coagulation and 2 min of flocculation at 110 rpm with a final pH between 7 and 8.6 ± 0.2; initial concentration of 5.0 ± 0.5 mg/L mg phosphorus/L.[36,37] Each data point represents an average of at least three separate jar test results and the error bar indicates standard error. *Indicates statistically significant difference ($p < 0.05$; two sample *t*-test) of contaminant removal when comparing ACH (orange) or ACH + pDADMAC (green) to alum. Selected data points for alum and ACH shown in (A, B) are sourced from the same dataset as Abi Farraj et al.[31]

the phosphorus removal declined with final concentrations reaching 1.17 ± 0.27 mg/L (removal of 77%) at pH 8.2 and 1.75 ± 0.03 mg/L (removal of 65%) at pH 8.6. Orthophosphate is known to be removed through direct adsorption on coagulant species or (co)precipitation with Al^{3+}.[49] At pH values above 8, phosphorus forms PO_3^{4-} and the lack of cationic aluminium-based species results in ineffective removal of phosphorus.[50] Therefore, the loss of cationic species at high pH conditions is seen to affect phosphorus and microfibre removal but does not impact nanoplastic removal at a longer settling time.

Although ACH-based coagulants were seen to improve contaminant removal at higher pH, ACH and ACH + pDADMAC showed poor phosphorus removal regardless of pH when compared to alum. The greater phosphorus removal with alum compared to ACH can be attributed to the high basicity of pre-hydrolyzed aluminium coagulants. ACH coagulant species contain hydroxyl groups that are strongly bound to Al, which prevents them from forming inner-sphere complexes with phosphates.[51] In contrast to alum, the lowest phosphorus concentration for these coagulants was achieved at the highest pH condition of 8.6 with a final concentration of 2.87 ± 0.09 mg/L (removal of 43%) and 2.56 ± 0.22 mg/L (removal of 49%) for ACH and ACH + pDADMAC, respectively. The improved removal of phosphorus at higher pH with ACH was also observed in previous work,[52] which was attributed to the lower overall

alkalinity at high pH which can improve precipitation efficiency of phosphate salts.[53] This finding highlights the complexity of contaminant removal through coagulation and flocculation, since different contaminants are removed via varying mechanisms; a coagulant that optimizes charge neutralization resulting in high nanoplastic removal can result in lower inner-sphere complexation thereby reducing phosphorus removal.

3.3 | Quartz crystal microbalance with dissipation monitoring study

Jar test experiments revealed that the three coagulants resulted in varying nanoplastic and microfibre removal. To better understand the differences in interactions of each coagulant with these plastic contaminants, quartz crystal microbalance with dissipation monitoring (QCM-D) was employed in this study. In the field of water treatment, QCM-D has recently provided useful insights into the mechanisms of coagulation and flocculation observed during primary treatment stages.[25,54,55] As an aqueous solution is flown over the sensor, QCM-D can provide valuable quantitative and qualitative information of hydrolyzed coagulant specie deposition on the sensor surface and properties of the deposited film. Information such as the film deposition rate and viscoelastic property can identify coagulant properties critical for high rates of nanoplastic and microfibre removal. Silica was selected as the sensor coating in these experiments as a representative negatively charged surface to enable us to better understand the nature of interaction between the coagulant with negatively charged particles such as Si-based colloids,[56] nanoplastics,[57] microplastics,[58] and microfibres.[59]

In QCM-D measurements, deposition on the crystal can be measured through monitoring the shifts of the crystal resonance frequency (Δf) allowing nanoscale mass to be detected.[60,61] Within the first 15 min of QCM-D measurements, alum shows minimal decrease in frequency shift (Figure 4A). This result indicates the alum hydrolyzed products at pH 7 do not yield large deposition on the sensor surface suggesting weak interactions between alum species and negatively charged SiO_2 surface. At pH 7, alum hydrolyses mostly into amorphous $Al(OH)_3$,[46] thus any deposition on the surface is likely due to the interaction of these amorphous products. On the other hand, ACH hydrolysis species at pH 8.5 showed a large negative frequency shift reaching an average value of approximately −80 Hz before the 15 min mark. The ACH species therefore resulted in large deposition on the sensor surface, indicating significantly stronger interactions with the sensor surface compared to alum. Nuclear magnetic resonance (NMR) spectra measurements showed that this ACH coagulant contains roughly 88% of polynuclear Al_{30}.[32] The positively charged aluminium species are stable at wide ranges of pH,[46] and therefore are expected to experience strong electrostatic interactions with the surface at pH 8.5. This result is in agreement with QCM-D measurements by Zhang al.[54] where Al_{30} deposition was mainly formed through particulate aluminium deposition resulting in a viscoelastic hydrated film. Similarly, Lapointe et al.[25] showed that alum species (containing $Al(OH)_3$), resulted in the lowest deposition rate while ACH (containing Al_{30} species)

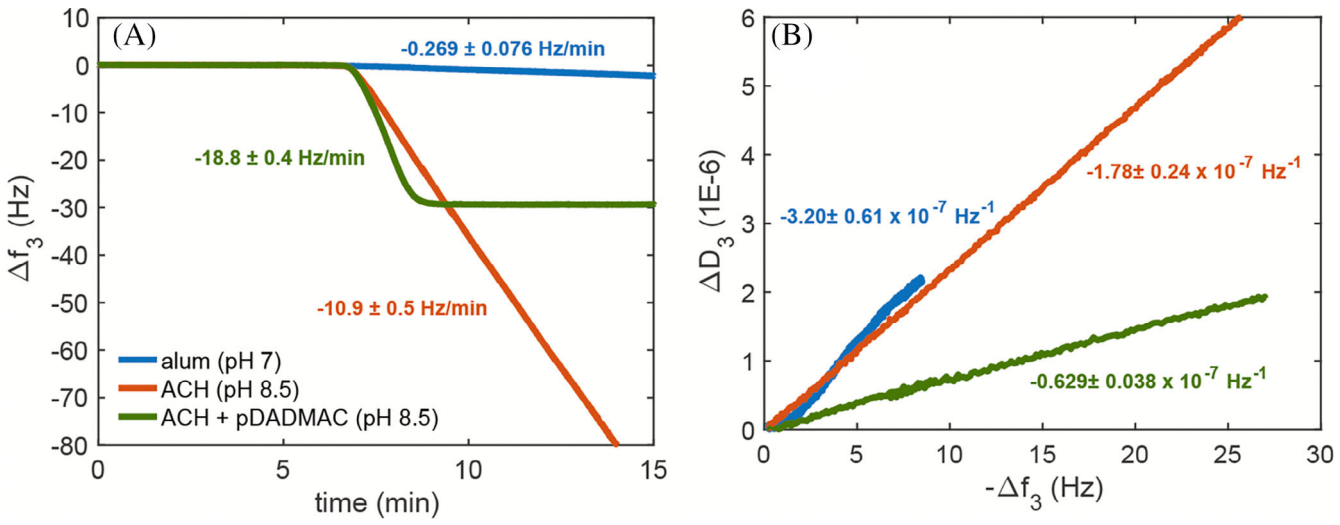

FIGURE 4 (A) Average frequency shift (Δf_3) versus time and (B) average change in dissipation (ΔD_3) versus the negative of the frequency shift ($-\Delta f_3$) for the deposition of alum (pH 7 ± 0.2), aluminium chlorohydrate (ACH) (pH 8.5 ± 0.2), and ACH + pDADMAC (pH 8.5 ± 0.2) with a concentration of 5.45 mg Al/L on crystals with silica-coated surfaces. Each line shows the average of three distinct measurements and the slopes are calculated based on the average slope of the three measurements with standard error shown.

resulted in greater deposition on weathered polystyrene surface. The addition of cationic pDADMAC with ACH resulted in the fastest deposition rate with a frequency shift rate of -18.8 ± 0.4 Hz/min compared to -10.9 ± 0.5 Hz/min and -0.269 ± 0.076 Hz/min for ACH and alum, respectively (Figure 4A). The deposition rate of ACH was still found to be 100× larger than that of alum when the calculated slopes were normalized with the theoretical deposition rate of the respective coagulation species according to the Smoluchowski-Levich approximation for a parallel-plate flow chamber.[62] Moreover, ACH + pDADMAC was the only coagulant to reach full surface saturation within 15 min of measurement. This result shows that the addition of pDADMAC significantly strengthens interaction between the coagulant and the negatively charged SiO_2 surface.

The viscoelastic properties of the deposited layer can be further evaluated by plotting the change in dissipation (ΔD) versus the change in frequency shift (Δf). A flat slope in the ΔD versus Δf plot indicates a rigid film with low energy dissipation per coupled-mass change, while a steep slope indicates a loosely bound film with high energy dissipation as the quantity of deposited material increases.[63] The least steep ΔD versus Δf slope (smallest slope magnitude) was measured for ACH + pDADMAC (Figure 4B) with a value of $-0.629 \pm 0.038 \times 10^{-7}$ Hz^{-1} showing that ACH + pDADMAC forms a more rigid film than both ACH (slope of $-1.78 \pm 0.24 \times 10^{-7}$ Hz^{-1}) and alum (slope of $-3.20 \pm 0.61 \times 10^{-7}$ Hz^{-1}). Therefore, the film of ACH + pDADMAC can be considered to have minimal dissipative losses and thus forms the most rigid layer out of the three coagulants. It should be noted that the average value of $\Delta D_n/(-\Delta f_n/n)$ obtained for all coagulants is below the empirical stiff-viscoelastic film limit ($4 \cdot 10^{-7}$ Hz^{-1})[64] which implies that all the tested coagulants form a relatively rigid film. In addition, frequency shifts at high overtones $\Delta f_{(n)}$ for all the tested coagulants are negative which serves as further evidence that all coagulants tested resulted in rigidly adsorbed films[65,66] (Figure S8).

The ΔD versus Δf plots for ACH and ACH + pDADMAC are linear throughout the measured frequency shifts, which indicates that the conformation of both deposited layers did not change during deposition. On the other hand, the measurements of ΔD versus Δf for alum reveal a nearly flat slope at the initial frequency shifts followed by an increase in the slope to reach an average of $-3.2 \pm 0.61 \cdot 10^{-7}$ Hz^{-1} (Figure 4B). The increase in slope indicates that the deposited layer became more loosely bound as the deposited material increased. This increase in ΔD versus Δf slope was also observed by Zhang et al.[54] for monomeric Al_0 species.

The QCM-D results above reveal mechanistic insights into the nanoplastic and microfibre removal behaviour of each coagulant. Effective nanoplastic removal can still be achieved with coagulants that result in less rigid, amorphous deposition (alum at pH 7; nanoplastic removal of $64 \pm 3\%$). The decline in nanoplastic removal at higher pH values using alum can be then explained by the increased production of soluble $Al(OH)_4^-$ species at the expense of the amorphous $Al(OH)_3$ deposits. At pH 8.6, ACH + pDADMAC was able to achieve a higher nanoplastic removal ($57 \pm 5\%$) compared to ACH ($33 \pm 9\%$). Although ACH had a higher deposition rate on the silica surface, the addition of pDADMAC resulted in a faster and more rigid film deposition. Therefore, the QCM-D study revealed that the improved nanoplastic removal with ACH + pDADMAC can be due to stronger and faster neutralizing behaviour due to the addition of pDADMAC. Despite the greater nanoplastic removal, ACH showed higher microfibre removal compared to ACH + pDADMAC at pH 8.6 ($95 \pm 1\%$ vs. $64 \pm 10\%$ respectively). While the rapid adsorption of a rigid layer by ACH + pDADMAC resulted in improved nanoplastic removal, this same film deposition behaviour can explain the lower microfibre removal at pH values above 8.2. The cationic pDADMAC can rapidly saturate negatively charged contaminants and flocculant loops preventing the bridging mechanism and therefore producing the small flocs. It has previously been shown that strong electrostatic interactions between flocculants and cationic species result in smaller floc sizes.[67] Therefore, the QCM-D results reveal that while fast and rigid film deposition is favourable for removing nanoplastic contaminants via charge neutralization, a rigid film can inhibit the formation of large flocs essential for removing microfibres via bridging mechanism.

3.4 | Testing nanoplastic removal with alternative flocculants

Flocculant properties, including molecular weight and charge density, are known to affect the formed flocs in a physicochemical treatment process.[68] Jar tests with anionic flocculants resulted in significantly larger floc sizes compared to cationic flocculants ($p < 0.005$ for aPAM1 and $p < 10^{-7}$ for aPAM2; Figure 5). Earlier studies have shown that electrostatic repulsion between anionic PAM and the negatively charged colloids in wastewater generally lead to the expansion of the polymer and consequently forms open-structure flocs that are larger than those produced by cationic flocculants.[68] A higher molecular weight of anionic polyacrylamide (aPAM2) also resulted in significantly larger average floc sizes ($p < 0.05$). At higher molecular weight and low to moderate charge density, PAM acts by bridging

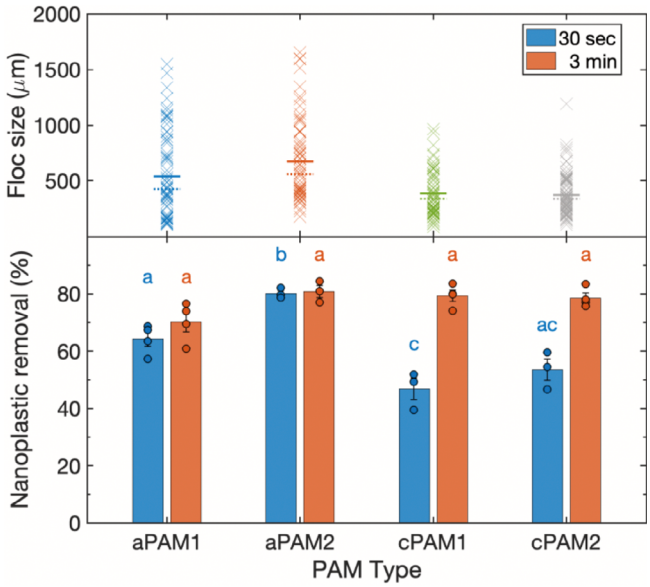

FIGURE 5 Floc size distribution of flocs formed with varying flocculant molecular weight and charge density. Solid line shows the mean size and the dashed line represents the median. Nanoplastic removal after 30 s of settling and 3 min of settling. 5.45 mg Al/L of alum as coagulant; aPAM1, aPAM2, cPAM1 or cPAM2 as flocculant (0.4 mg PAM/L); 2 min of coagulation and 2 min of flocculation at 110 rpm with a final pH of 7 ± 0.2. aPAM1: Very low anionic charge density, high molecular weight; aPAM2: Very low anionic charge density, very high molecular weight; cPAM1: Very low cationic charge density, high molecular weight; cPAM2: Low cationic charge density, high molecular weight. Statistical significance is shown as $p < 0.05$ (two sample *t*-test). The nanoplastic removal results presented above are sourced from the same dataset as Abi Farraj et al.[31]

mechanism, while charge neutralization is considered relatively insignificant.[69] Therefore, higher molecular weight polymers can improve the bridging flocculation resulting in larger floc sizes. The anionic polymer with larger floc sizes also resulted in a greater nanoplastic removal at short settling time of 30 s ($p = 0.004$) as well as longer settling time of 3 min (although not statistically significant; $p = 0.065$) (Figure 5). This finding reveals that floc size can play a critical role in removal of nano-sized contaminants during the coagulation and flocculation process. The role of floc size in nanoplastic removal was also seen in a recent coagulation and flocculation study where screening was used for floc separation.[70] Using the smallest mesh size of 1000 μm, nanoplastic removal in jar tests performed with only alum and flocculant (mean floc size = 520 ± 50 μm; 82% nanoplastic removal) was significantly lower than jar tests performed with super-bridging fibres (mean floc size >3930 μm; 94% nanoplastic removal). This finding further confirms the critical role that floc size plays in improving nanoplastic removal during coagulation particularly through enhancing removal via sweep flocculation. This finding further shows that orthokinetic flocculation is the dominant collision mechanism during coagulation and flocculation as first demonstrated in our earlier work.[31] Since the rate constant of orthokinetic flocculation is proportional to third power of the floc size,[71] aPAM2 can result in much faster collisions of nanoplastics with flocs.

Cationic polyacrylamides, regardless of charge density, showed lower overall removal compared to both anionic polyacrylamides for samples taken after 30 s of settling (Figure 5). Cationic polyacrylamides do not result in strong bridging mechanisms since the electrostatic interaction between the flocculants and the colloids results in strong adsorption and consequently smaller floc sizes.[67] These smaller flocs require longer settling times which explains the lower nanoplastic removal seen after only 30 s of settling. Even though cPAM1 and cPAM2 also had a smaller floc size distribution compared to aPAM2, the cationic flocculants no longer show a significant difference in nanoplastic removal compared to anionic flocculants at the longer settling time of 3 min ($p > 0.05$). Given sufficiently long settling time, the cationic flocculants can compensate for the smaller flocs produced. It is likely that the improved attachment efficiency due to the enhanced destabilization of the negatively charged nanoplastics by the cationic flocculants can compensate for lower collision rates of the smaller flocs. Interestingly, increasing the charge density of the cationic flocculant from ~7% (cPAM1) to ~20% (cPAM2) did not result in a significant change in nanoplastic removal at either 30 s or 3 min settling times. This finding suggests that sufficient cationic sites were already provided by the cPAM with 7% charge density to allow nanoplastic aggregation. The results above suggest that both cationic and anionic flocculants can be used by wastewater treatment plant operators to achieve similar nanoplastic removal efficiencies given sufficient settling time. However, anionic flocculants with very high molecular weight flocculants (such as aPAM2) provide optimal nanoplastic removal for wastewater treatment plants that operate with high flowrates and are restricted to short settling times.

4 | CONCLUSION

In this study, the removal of nanoplastics and microfibres with conventional and alternative aluminium-based coagulants is investigated during physicochemical treatment. Using alum as a coagulant removes 97% of microfibres at an optimal pH of 7; however increasing the pH to 8.6 resulted in a significant decline of removal reaching 85%. Similarly, nanoplastic removal with alum after 30 s of settling decreases from 64% to approximately 0%

removal when the pH is increased from 7 to 8.6. This is an important observation as several wastewater treatment plants globally operate at pH >8—systematically or occasionally. In these challenging operating conditions, our results reveal that the addition of cationic species to the coagulant result in improved nanoplastic removal after settling (30 s): 10% for alum alone, 52% for ACH, and 68% for ACH + pDADMAC (pH 7.5–8.5). Similarly, ACH results in a greater microfibre removal compared to alum (94% vs. 86% average removal for pH >8, respectively). QCM-D results suggest that alum interacts with negatively charged colloids through amorphous $Al(OH)_3$ deposition. The dissipation shift measurements reveal that both ACH and alum formed less rigid films, while the addition of pDADMAC resulted in a highly rigid film deposited on the negatively charged surface. The behaviour of nanoplastic removal during physicochemical treatment was also revealed through this study. After 3 min of settling, there was no observed difference in nanoplastic removal with alum in alkaline conditions (pH >8) which reveals that longer settling time can compensate for loss of cationic coagulant species when sweep flocculation dominates the coagulation process. Nanoplastic removal with different flocculants further highlights this result where increasing cationic charge density did not lead to significantly greater nanoplastic removal. This study improves our understanding of surface interactions of the coagulants with plastic surfaces in relevant environmental conditions. More importantly, this study offers municipalities new solutions in coagulation to better remove nanosized plastic pollution.

AUTHOR CONTRIBUTIONS

Sinan Abi Farraj: Conceptualization; investigation; writing – original draft; methodology; validation; visualization; formal analysis; data curation. **Mathieu Lapointe:** Writing – review and editing; validation; visualization; supervision; formal analysis; investigation; methodology. **Rafael S. Kurusu:** Validation; writing – review and editing; investigation. **Nathalie Tufenkji:** Funding acquisition; validation; writing – review and editing; supervision; resources; project administration.

ACKNOWLEDGEMENTS

The authors acknowledge the Canada Research Chairs Program [CRC-2022-00274], the Natural Sciences and Engineering Research Council of Canada (NSERC) [RGPAS-2019-00117 and RGPIN-2019-04519], and the Canada Foundation for Innovation [217263, 36368, 40070, 43152]. S.A.F. was supported by a Graduate Excellence Fellowship at McGill, M.L. was supported by a Mitacs Accelerate Fellowship and Kemira Water Solutions Canada Inc., and R.S.K. was supported by NSERC and FRQNT Postdoctoral Fellowships.

PEER REVIEW

The peer review history for this article is available at https://www.webofscience.com/api/gateway/wos/peer-review/10.1002/cjce.70235.

DATA AVAILABILITY STATEMENT

The data that support the findings of this study are available from the corresponding author upon reasonable request.

REFERENCES

[1] J. C. Anderson, B. J. Park, V. P. Palace, *Environ. Pollut.* **2016**, *218*, 269.
[2] J.-W. Jung, J.-W. Park, S. Eo, J. Choi, Y. K. Song, Y. Cho, S. H. Hong, W. J. Shim, *Environ. Pollut.* **2021**, *270*, 116217.
[3] A. R. A. Lima, M. Barletta, M. F. Costa, *Estuar. Coast. Shelf Sci.* **2015**, *165*, 213.
[4] C. M. Free, O. P. Jensen, S. A. Mason, M. Eriksen, N. J. Williamson, B. Boldgiv, *Mar. Pollut. Bull.* **2014**, *85*, 156.
[5] C. Bertoldi, L. Z. Lara, A. d. L. Fernanda, F. C. G. Martins, M. A. Battisti, R. Hinrichs, A. N. Fernandes, *Sci. Total Environ.* **2021**, *759*, 143503.
[6] W. Luo, L. Su, N. J. Craig, F. Du, C. Wu, H. Shi, *Environ. Pollut.* **2019**, *246*, 174.
[7] S. M. Mintenig, M. G. J. Löder, S. Primpke, G. Gerdts, *Sci. Total Environ.* **2019**, *648*, 631.
[8] J. Sun, X. Dai, Q. Wang, M. C. M. van Loosdrecht, B.-J. Ni, *Water Res.* **2019**, *152*, 21.
[9] A. L. Andrady, *Mar. Pollut. Bull.* **2011**, *62*, 1596.
[10] M. A. Browne, P. Crump, S. J. Niven, E. Teuten, A. Tonkin, T. Galloway, R. Thompson, *Environ. Sci. Technol.* **2011**, *45*, 9175.
[11] A. A. Horton, A. Walton, D. J. Spurgeon, E. Lahive, C. Svendsen, *Sci. Total Environ.* **2017**, *586*, 127.
[12] M. L. Pedrotti, S. Petit, B. Eyheraguibel, M. E. Kerros, A. Elineau, J. F. Ghiglione, J. F. Loret, A. Rostan, G. Gorsky, *Sci. Total Environ.* **2021**, *758*, 144195.
[13] O. Pikuda, M. Lapointe, O. S. Alimi, D. Berk, N. Tufenkji, *J. Hazard. Mater.* **2022**, *438*, 129408.
[14] J. Boucher, D. Friot, *Primary Microplastics in the Oceans: A Global Evaluation of Sources*, IUCN, Gland, Switzerland **2017**.
[15] O. S. Alimi, D. Claveau-Mallet, R. S. Kurusu, M. Lapointe, S. Bayen, N. Tufenkji, *J. Hazard. Mater.* **2021**, *423*(Part A), 126955. https://doi.org/10.1016/j.jhazmat.2021.126955
[16] A. Jahnke, H. P. H. Arp, B. I. Escher, B. Gewert, E. Gorokhova, D. Kühnel, M. Ogonowski, A. Potthoff, C. Rummel, M. Schmitt-Jansen, *Environ. Sci. Technol. Lett.* **2017**, *4*, 85.
[17] T. Yang, J. Luo, B. Nowack, *Environ. Sci. Technol.* **2021**, *55*, 15873.
[18] J. Gigault, B. Pedrono, B. Maxit, A. Ter Halle, *Environ. Sci.: Nano* **2016**, *3*, 346.
[19] M. T. Ekvall, M. Lundqvist, E. Kelpsiene, E. Šileikis, S. B. Gunnarsson, T. Cedervall, *Nanoscale Adv.* **2019**, *1*, 1055.
[20] L. M. Hernandez, N. Yousefi, N. Tufenkji, *Environ. Sci. Technol. Lett.* **2017**, *4*, 280.
[21] International Standard Organization, *ISO/TR 21960:2020 Plastics — Environmental aspects — State of Knowledge and Methodologies* (ISO Technical Reports 21960:2020), 1st ed., International Standard Organization, Geneva, Switzerland **2020**.
[22] A. Ter Halle, J. F. Ghiglione, *Environ. Sci. Technol.* **2021**, *55*, 14466.
[23] J. Gigault, H. El Hadri, B. Nguyen, B. Grassl, L. Rowenczyk, N. Tufenkji, S. Feng, M. Wiesner, *Nat. Nanotechnol.* **2021**, *16*, 501.

[24] P. Pal, in *Industrial Water Treatment Process Technology* (Ed: P. Pal), Butterworth-Heinemann, Oxford, UK **2017**, p. 243.
[25] M. Lapointe, J. M. Farner, L. M. Hernandez, N. Tufenkji, *Environ. Sci. Technol.* **2020**, *54*, 8719.
[26] J. Li, M. Dagnew, M. B. Ray, *Environ. Res.* **2022**, *212*, 113401.
[27] Y. Gong, Y. Bai, D. Zhao, Q. Wang, *Water Res.* **2021**, *208*, 117884.
[28] Y. Zhang, X. Wang, Y. Li, H. Wang, Y. Shi, Y. Li, Y. Zhang, *J. Hazard. Mater.* **2021**, *425*, 127962.
[29] Ministère De l'Environnement Et De La Lutte Contre Les Changements Climatiques, *Règlements sur les ouvrages municipaux d'assainissements des eaux usées, RLRQ, c. Q-2, r. 34.1*, Ministère de l'Environnement et de la Lutte contre les Changements Climatiques, Québec, Canada **2013**.
[30] B. Ma, W. Xue, C. Hu, H. Liu, J. Qu, L. Li, *Chem. Eng. J.* **2019**, *359*, 159.
[31] S. Abi Farraj, M. Lapointe, R. S. Kurusu, Z. Liu, B. Barbeau, N. Tufenkji, *Nature Water* **2024**, *2*, 72.
[32] M. Lapointe, I. Papineau, S. Peldszus, N. Peleato, B. Barbeau, *J. Water Process Eng.* **2021**, *40*, 101829.
[33] Organisation for Economic Cooperation & Development, *Test No. 303: Simulation Test-Aerobic Sewage Treatment–A: Activated Sludge Units; B: Biofilms*, OECD Publishing, Paris, France **2001**.
[34] Canadian Council of Ministers of the Environment, in *Canadian Water Quality Guidelines for the Protection of Aquatic Life: Phosphorus: Canadian Guidance Framework for the Management of Freshwater Systems* (Ed: Canadian Council of Ministers of the Environment Winnipeg) Canadian Council of the Ministers of the Environment, Winnipeg, Canada **2004**.
[35] J. Z. Ross, S. Omelon, *Facets* **2018**, *3*, 642.
[36] M. Lapointe, R. S. Kurusu, L. M. Hernandez, N. Tufenkji, *ACS ES&T Water* **2023**, *3*, 377.
[37] R. S. Kurusu, M. Lapointe, N. Tufenkji, *Chem. Eng. J.* **2022**, *430*, 132927.
[38] C. P. Johnson, X. Li, B. E. Logan, *Environ. Sci. Technol.* **1996**, *30*, 1911.
[39] M. O. Akanbi, L. M. Hernandez, M. H. Mobarok, J. G. C. Veinot, N. Tufenkji, *Environ. Sci.: Nano* **2018**, *5*, 2172.
[40] *MATLAB and Optimization Toolbox (R2022b)*, The MathWorks Inc., Natick, MA **2022**.
[41] J. C. Crittenden, R. R. Trussell, D. W. Hand, K. J. Howe, G. Tchobanoglous, *MWH's Water Treatment: Principles and Design*, John Wiley & Sons, Hoboken, NJ **2012**.
[42] P. L. Hayden, A. J. Rubin, in *Aqueous Environmental Chemistry of Metal* (Ed: A. J. Rubin), Ann Arbor Science Publishers, Ann Arbor, MA **1974**, p. 318.
[43] Z. L. Yang, B. Y. Gao, Q. Y. Yue, Y. Wang, *J. Hazard. Mater.* **2010**, *178*, 596.
[44] N. K. Shahi, M. Maeng, D. Kim, S. Dockko, *Process Saf. Environ. Prot.* **2020**, *141*, 9.
[45] W. Liu, J. Zhang, H. Liu, X. Guo, X. Zhang, X. Yao, Z. Cao, T. Zhang, *Environ. Int.* **2021**, *146*, 106277.
[46] O. P. Sahu, P. K. Chaudhari, *J. Appl. Sci. Environ. Manage.* **2013**, *17*, 241.
[47] Z. Chen, B. Fan, X. Peng, Z. Zhang, J. Fan, Z. Luan, *Chemosphere* **2006**, *64*, 912.
[48] K. Rajala, O. Grönfors, M. Hesampour, A. Mikola, *Water Res.* **2020**, *183*, 116045.
[49] M. Aguilar, J. Saez, M. Llorens, A. Soler, J. Ortuno, *Water Res.* **2002**, *36*, 2910.
[50] D. Georgantas, H. Grigoropoulou, *J. Colloid Interface Sci.* **2007**, *315*, 70.
[51] B. Wu, J. Wan, Y. Zhang, B. Pan, I. M. Lo, *Environ. Sci. Technol.* **2019**, *54*, 50.
[52] C. Mancuso, M. Jamison, J. Zaporski, Z. Yang, *Water Environ. Res.* **2021**, *93*, 2589.
[53] T. Zhang, L. Ding, H. Ren, Z. Guo, J. Tan, *J. Hazard. Mater.* **2010**, *176*, 444.
[54] Y. Zhang, B. Shi, Y. Zhao, M. Yan, D. A. Lytle, D. Wang, *J. Environ. Sci.* **2016**, *42*, 142.
[55] W. Wu, J. Ma, J. Xu, Z. Wang, *Chem. Eng. J.* **2021**, *410*, 128425.
[56] J. Bratby, *Coagulation and Flocculation in Water and Wastewater Treatment*, IWA Publishing, London, England **2016**.
[57] M. Sarcletti, H. Park, J. Wirth, S. Englisch, A. Eigen, D. Drobek, D. Vivod, B. Friedrich, R. Tietze, C. Alexiou, *Mater. Today* **2021**, *48*, 38.
[58] S. Lu, K. Zhu, W. Song, G. Song, D. Chen, T. Hayat, N. S. Alharbi, C. Chen, Y. Sun, *Sci. Total Environ.* **2018**, *630*, 951.
[59] G. Agarwal, A. Perwuelz, L. Koehl, K. S. Lee, *J. Surfactants Deterg.* **2012**, *15*, 97.
[60] Q. Chen, S. Xu, Q. Liu, J. Masliyah, Z. Xu, *Adv. Colloid Interface Sci.* **2016**, *233*, 94.
[61] G. Liu, G. Zhang, *QCM-D Studies on Polymer Behavior at Interfaces*, Springer, New York **2013**, p. 1.
[62] I. R. Quevedo, N. Tufenkji, *Environ. Sci. Technol.* **2009**, *43*, 3176.
[63] W. Li, D. Liu, J. Wu, C. Kim, J. D. Fortner, *Environ. Sci. Technol.* **2014**, *48*, 11892.
[64] I. Reviakine, D. Johannsmann, R. P. Richter, *Anal. Chem.* **2011**, *83*, 8838.
[65] A. L. J. Olsson, H. C. van der Mei, D. Johannsmann, H. J. Busscher, P. K. Sharma, *Anal. Chem.* **2012**, *84*, 4504.
[66] I. R. Quevedo, A. L. J. Olsson, R. J. Clark, J. G. C. Veinot, N. Tufenkji, *Environ. Eng. Sci.* **2014**, *31*, 326.
[67] M. Lapointe, B. Barbeau, *Sep. Purif. Technol.* **2020**, *231*, 115893.
[68] M. S. Nasser, A. E. James, *Sep. Purif. Technol.* **2006**, *52*, 241.
[69] M. Patience, J. Addai-Menash, J. Ralston, *Int. J. Miner. Process.* **2003**, *71*, 247.
[70] M. Lapointe, H. Jahandideh, J. M. Farner, N. Tufenkji, *NPJ Clean Water* **2022**, *5*, 11.
[71] C. R. O'Melia, in *The Scientific Basis of Flocculation* (Ed: K. J. Ives), Springer, Cambridge, UK **1978**, p. 219.

SUPPORTING INFORMATION

Additional supporting information can be found online in the Supporting Information section at the end of this article.

How to cite this article: S. Abi Farraj, M. Lapointe, R. S. Kurusu, N. Tufenkji, *Can. J. Chem. Eng.* **2026**, 1. https://doi.org/10.1002/cjce.70235